

INFECTIOUS DISEASE

Rapid profiling of RSV antibody repertoires from the memory B cells of naturally infected adult donors

2016 © The Authors,
some rights reserved;
exclusive licensee
American Association
for the Advancement
of Science.

Morgan S. A. Gilman,^{1*} Carlos A. Castellanos,^{2*} Man Chen,³ Joan O. Ngwuta,³ Eileen Goodwin,² Syed M. Moin,³ Vicente Mas,⁴ José A. Melero,⁴ Peter F. Wright,⁵ Barney S. Graham,³ Jason S. McLellan,¹ Laura M. Walker^{2†}

Respiratory syncytial virus (RSV) causes substantial morbidity and mortality in young children and the elderly. There are currently no licensed RSV vaccines, and passive prophylaxis with the monoclonal antibody palivizumab is restricted to high-risk infants in part due to its modest efficacy. Although it is widely agreed that an effective RSV vaccine will require the induction of a potent neutralizing antibody response against the RSV fusion (F) glycoprotein, little is known about the specificities and functional activities of RSV F-specific antibodies induced by natural infection. We have comprehensively profiled the human antibody response to RSV F by isolating and characterizing 364 RSV F-specific monoclonal antibodies from the memory B cells of three healthy adult donors. In all donors, the antibody response to RSV F was composed of a broad diversity of clones that targeted several antigenic sites. Nearly half of the most potent antibodies targeted a previously undefined site of vulnerability near the apex of the pre-fusion conformation of RSV F (preF). Additionally, the antibodies targeting this new site displayed convergent sequence features, thus providing a future means to rapidly detect the presence of these antibodies in human vaccine samples. Many of the antibodies that bind preF-specific surfaces were >100 times more potent than palivizumab and several cross-neutralized human metapneumovirus. Together, the results have implications for the design and evaluation of RSV vaccine candidates and offer new options for passive prophylaxis.

INTRODUCTION

Respiratory syncytial virus (RSV) is the leading cause of infant hospitalization in the United States and accounts for an estimated 64 million infections and 160,000 deaths worldwide each year. However, despite decades of research, the development of a safe and effective vaccine against RSV has remained elusive, highlighting the need for novel strategies that induce protective immune responses. Neutralizing antibodies have been shown to protect against severe RSV disease in humans and animal models; therefore, it is widely agreed that an effective RSV vaccine should induce a robust neutralizing antibody response (1–3).

Similar to other pneumoviruses, RSV expresses two major surface glycoproteins: the fusion protein (F) and the attachment protein (G). Although both have been shown to induce protective neutralizing antibody responses, F is less genetically variable than G, is absolutely required for infection, and is the target for the majority of neutralizing activity in human serum (4–8). RSV F is also the target of the monoclonal antibody (mAb) palivizumab, which is used to passively protect high-risk infants from severe disease (9). Consequently, the RSV F protein is considered to be a highly attractive target for vaccines and antibody-based therapies.

The mature RSV F glycoprotein initially exists in a metastable pre-fusion conformation (preF) (10) before undergoing a conformational change that leads to insertion of the hydrophobic fusion peptide into the host-cell membrane. Subsequent refolding of F into a stable,

elongated postfusion conformation (postF) (11, 12) results in fusion of the viral and host-cell membranes. Because of its inherent instability, the preF protein has the propensity to prematurely trigger into postF, both in solution and on the viral surface (13). Recently, stabilization of preF has been achieved by protein engineering (14, 15), and stabilized preF has been shown to induce higher titers of neutralizing antibodies than postF in animal models (14, 15).

Despite the importance of neutralizing antibodies in protection against severe RSV disease, our understanding of the human antibody response to RSV has been limited to studies of human sera and a small number of RSV-specific human mAbs (16–19). The epitopes recognized by these human antibodies, as well as several murine antibodies, have defined at least four “antigenic sites” on RSV F (table S1) (1, 10, 16, 18–20). Three of these sites—I, II, and IV—are present on both preF and postF, whereas antigenic site Ø exists exclusively on preF. Additional preF-specific epitopes have been defined by antibodies MPE8 (17) and AM14 (21). Although serum-mapping studies have shown that site Ø-directed antibodies are responsible for a large proportion of the neutralizing antibody response in most individuals (8), there are additional antibody specificities that contribute to serum-neutralizing activity that remain to be defined. In addition, it is unknown whether certain antibody sequence features are required for recognition of certain neutralizing sites, as observed for other viral targets (22–25). Last, understanding the relationship between neutralization potency and epitope specificity will be critical in the selection and design of vaccine antigens that induce potent neutralizing responses.

To address these questions, we isolated an extensive panel of RSV F-specific mAbs from the memory B cells of three healthy adult donors and used these antibodies to comprehensively map the antigenic topology of RSV F. The results show that a large proportion of the RSV F-specific human antibody repertoire is composed of neutralizing antibodies, many of which exhibit marked potency. The most potent antibodies target two distinct antigenic sites that are located near the apex of the preF trimer, providing strong support for the development

¹Department of Biochemistry and Cell Biology, Geisel School of Medicine at Dartmouth, Hanover, NH 03755, USA. ²Adimab LLC, Lebanon, NH 03766, USA. ³Vaccine Research Center, National Institute of Allergy and Infectious Diseases, National Institutes of Health, Bethesda, MD 20892, USA. ⁴Centro Nacional de Microbiología and CIBER de Enfermedades Respiratorias, Instituto de Salud Carlos III, Majadahonda, Madrid, Spain. ⁵Department of Pediatrics, Geisel School of Medicine at Dartmouth, Hanover, NH 03755, USA.

*These authors contributed equally to this work.

†Corresponding author. Email: laura.walker@adimab.com

of preF-based vaccine candidates that preserve these antigenic sites. Furthermore, the highly potent neutralizing antibodies described here represent new opportunities for the prevention of severe RSV disease by passive immunoprophylaxis.

RESULTS

Large-scale isolation of RSV F-specific mAbs from healthy adult donors

To comprehensively profile the human antibody response to RSV F, we aimed to isolate and characterize about 100 mAbs from the memory B cells of each of three healthy adult donors. Although these donors did not have a documented history of RSV infection, healthy adults are expected to have had multiple RSV infections throughout life (26). We assessed the magnitude of the memory B cell response to RSV F by staining peripheral B cells with a mixture of fluorescently labeled preF and postF sorting probes (fig. S1) (11, 15). Both proteins were dual labeled to eliminate background due to non-specific fluorochrome binding (27). Flow cytometric analysis revealed that 0.04 to 0.18% of class-switched [immunoglobulin G-positive (IgG^+) and IgA^+] peripheral B cells were specific for RSV F (Fig. 1A and fig. S2), which is substantially lower than the percentage of RSV F-specific cells observed after experimental RSV infection, suggesting that these three donors were probably not recently exposed to RSV (28). Index sorting showed that 17 to 38% of circulating RSV F-specific B cells express IgA, indicating that IgA memory B cells to RSV F are present in peripheral blood (Fig. 1B). About 200 RSV F-specific B cells from each donor sample were single-cell sorted, and antibody variable heavy (VH) and variable light (VL) chain sequences were rescued by single-cell polymerase chain reaction (PCR) (29). More than 100 cognate heavy and light chain pairs from each donor were subsequently cloned and expressed as full-length IgGs in an engineered strain of *Saccharomyces cerevisiae* for further characterization (30). Preliminary binding studies showed that about 80% of antibodies cloned from RSV F-specific B cells bound to recombinant RSV F proteins (table S2).

Sequence analysis of RSV F-specific antibody repertoires

Sequence analysis of the isolated mAbs revealed that all three RSV F-specific repertoires were highly diverse, with each containing between 70 and 98 unique lineages (Fig. 1C and data file S1). This result is in stark contrast to the relatively restricted repertoires observed in HIV-infected patients (31) or in healthy donors after influenza vaccination (32). Compared with non-RSV-reactive antibodies (33), the RSV F-specific repertoires were skewed toward certain VH germline genes (*VH1-18*, *VH1-2*, *VH1-69*, *VH2-70*, *VH4-304*, and *VH5-51*) (Fig. 1D). A bias toward *VH1-69* has also been observed in anti-HIV-1, anti-influenza, and anti-hepatitis C virus repertoires (34–36), and recent studies have shown that there is a significant increase in the relative usage of *VH1-18*, *VH1-2*, and *VH1-69* during acute dengue infection (37). Hence, it appears that these particular germline gene segments may have inherent properties that facilitate recognition of viral envelope proteins. The distribution of heavy chain third complementarity-determining region (CDRH3) lengths in RSV F-specific antibody repertoires was skewed toward lengths of 14 to 18 amino acids compared with unselected repertoires (Fig. 1E). The average level of somatic hypermutation (SHM) varied between the three donor repertoires, ranging from 16 to 30 nucleotide substitutions per VH gene (excluding CDRH3) (Fig. 1F), which is comparable to the

average level of SHM observed in anti-influenza antibody repertoires (32, 38) and consistent with the recurrent nature of RSV infection (26). Several antibodies contained greater than 50 VH gene nucleotide substitutions, suggesting that multiple rounds of RSV infection can result in antibodies with very high levels of SHM.

A large proportion of antibodies bind exclusively to preF

We next measured the apparent binding affinities of the IgGs to furin-cleaved RSV F ectodomains stabilized in the prefusion (DS-Cav1) or postfusion (F ΔFP) conformation using biolayer interferometry (11, 15). In all three donor repertoires, a relatively large proportion of the antibodies (36 to 67%) bound exclusively to preF (Fig. 2, A and B). The vast majority of remaining antibodies bound to both preF and postF, with only 5 to 7% of antibodies showing exclusive postF specificity (Fig. 2, A and B). The low prevalence of postF-specific antibodies in these donor repertoires is consistent with the observation that less than 10% of anti-RSV F serum binding activity specifically targets postF (8). However, the majority of cross-reactive antibodies bound with higher apparent affinity to postF (Fig. 2A), suggesting that these antibodies were probably elicited by and/or affinity-matured against postF in vivo. Hence, the significantly higher proportion of preF- versus postF-specific antibodies is likely due to the higher immunogenicity of the unique surfaces on preF compared with postF, rather than to an increased abundance of preF in vivo. As expected based on the relatively high degree of sequence conservation of RSV F proteins, most of the antibodies bound to F proteins derived from subtypes A and B (Fig. 2C).

Because certain antiviral antibody specificities have been associated with poly- and autoreactivity (39–41), we also tested the RSV antibodies for polyreactivity using a previously described high-throughput assay that correlates with downstream behaviors such as serum clearance (42, 43). One hundred and seventy-seven clinical antibodies, as well as several broadly neutralizing HIV-1 antibodies, were also included for comparison. In contrast to many previously described HIV-1 broadly neutralizing antibodies, the vast majority of RSV F-specific antibodies lacked substantial polyreactivity in this assay (fig. S3).

RSV F-specific antibodies target six major antigenic sites

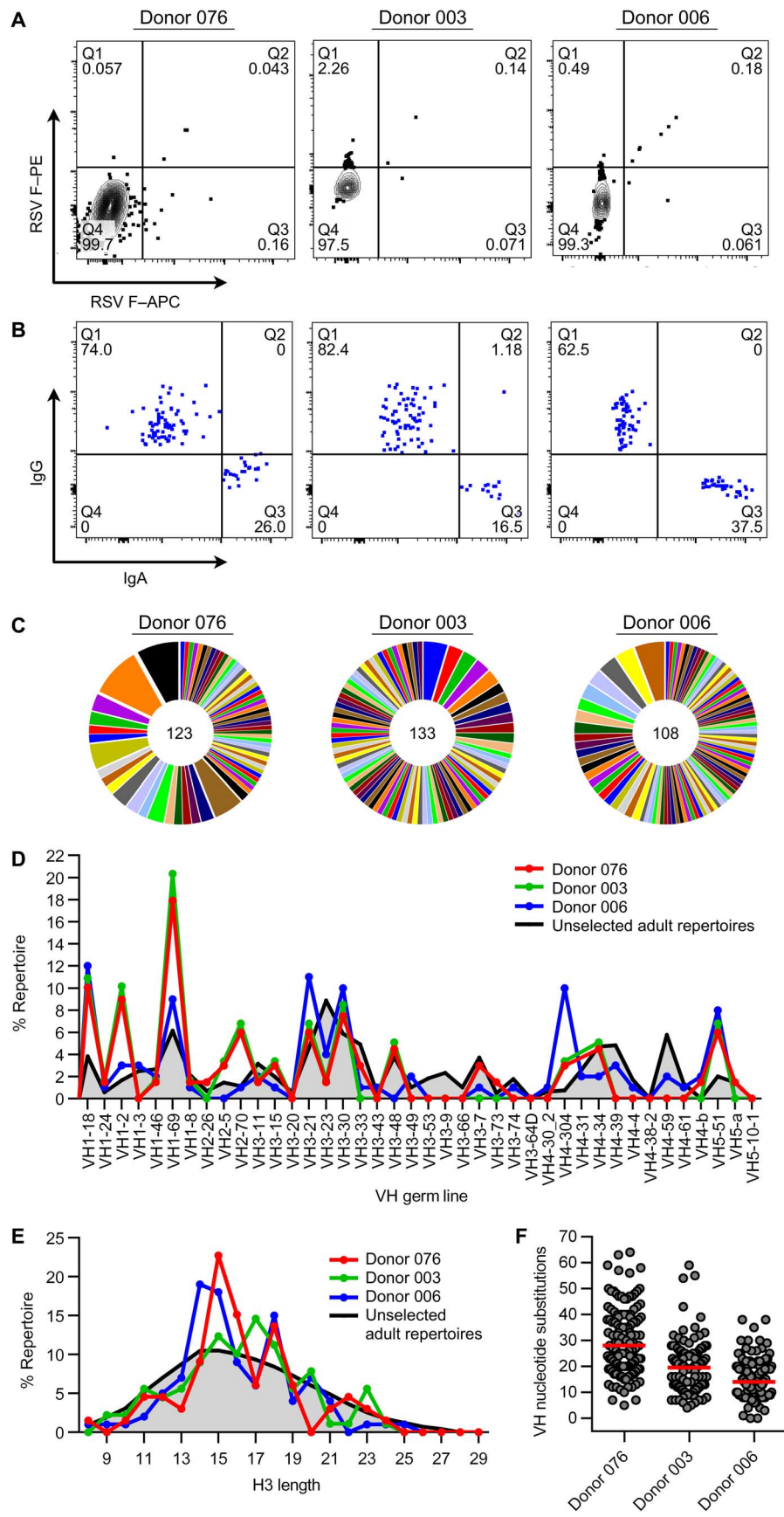
To map the epitopes recognized by the RSV F-specific antibodies, we first performed competitive binding experiments using a previously described yeast-based assay (44). Antibodies were initially tested for competition with D25, AM14, and MPE8 [three previously described preF-specific antibodies (10, 17, 21)] and motavizumab [an affinity-matured variant of palivizumab that binds to both preF and postF (10, 11, 45)]. Noncompeting antibodies were then tested for competition with a site IV-directed mAb (101F) (46), a site I-directed antibody (ADI-13390) (table S3), and two high-affinity antibodies from the panel (ADI-14443 and ADI-14469) that did not strongly compete with each other or any of the control antibodies (table S3). Each antibody was assigned to a bin based on the results of this competition assay (data file S1).

To increase the resolution of our epitope assignments, we also measured the binding of each antibody to a panel of preF variants using a Luminex-based assay (data file S1). Each variant contained two to four mutations clustered together to form a patch on the surface of preF. A total of nine patches that uniformly covered the surface of preF were generated (fig. S4). Deglycosylated preF was also included to identify antibodies targeting glycan-dependent epitopes.

Fig. 1. Anti-RSV F repertoire cloning. (A) RSV F-specific B cell sorting. Fluorescence-activated cell sorting plots show RSV F reactivity of IgG⁺ and IgA⁺ B cells from three healthy adult donors. B cells in quadrant 2 (Q2) were single cell-sorted. APC, allophycocyanin. (B) Isotype analysis. Index sort plots show the percentage of RSV F-specific B cells that express IgG or IgA. (C) Clonal lineage analysis. Each slice represents one clonal lineage; the size of the slice is proportional to the number of clones in the lineage. The total number of clones is shown in the center of the pie. Lineage numbering can be found in data file S1. Clonal lineages were assigned based on the following criteria: (i) matching of variable and joining gene segments, (ii) identical CDRH3 lengths, and (iii) >80% homology in CDRH3 nucleotide sequences. (D) VH repertoire analysis. VH germline genes were considered to be enriched in RSV repertoires if at least two of the three donors showed more than three-fold enrichment over non-RSV-specific repertoires (33). (E) CDRH3 length distribution. (F) SHM in VH (excluding CDRH3). Red bars indicate the median number of nucleotide substitutions. Each clonal lineage is only represented once in (D) and (E). Data for non-RSV-reactive IgGs were derived from published sequences obtained by high-throughput sequencing of rearranged antibody variable gene repertoires from healthy individuals (33).

Previously characterized antibodies D25, AM14, and motavizumab were used to validate the assay (fig. S4). The combined bin and patch data were then used to assign each antibody to a single antigenic site (Fig. 3, A and B), which we defined on the basis of previously determined structures, resistance mutations, and secondary structure of the F protein. Overall, these data show that the large majority of isolated antibodies target six major antigenic sites on prefusion RSV F (\emptyset , I, II, III, IV, and V). Only a small proportion of the isolated antibodies had binding profiles similar to that of AM14, suggesting that antibodies targeting this quaternary epitope are not commonly elicited during natural infection. None of the antibodies was sensitive to deglycosylation of F, demonstrating that glycan-dependent antibodies are also rarely elicited by natural RSV infection. All three donor repertoires showed highly similar epitope coverage, suggesting that the majority of healthy adults produce antibodies targeting each of these six antigenic sites.

Analysis of the preF- and postF-binding activities of the antibodies targeting each antigenic site (Fig. 3C and fig. S5) revealed that three sites are almost exclusively found on preF (\emptyset , III, and V). Antibodies targeting sites \emptyset and III have been previously described (10, 17), and these sites are located on the top and side of the preF protein, respectively. Between 4 and



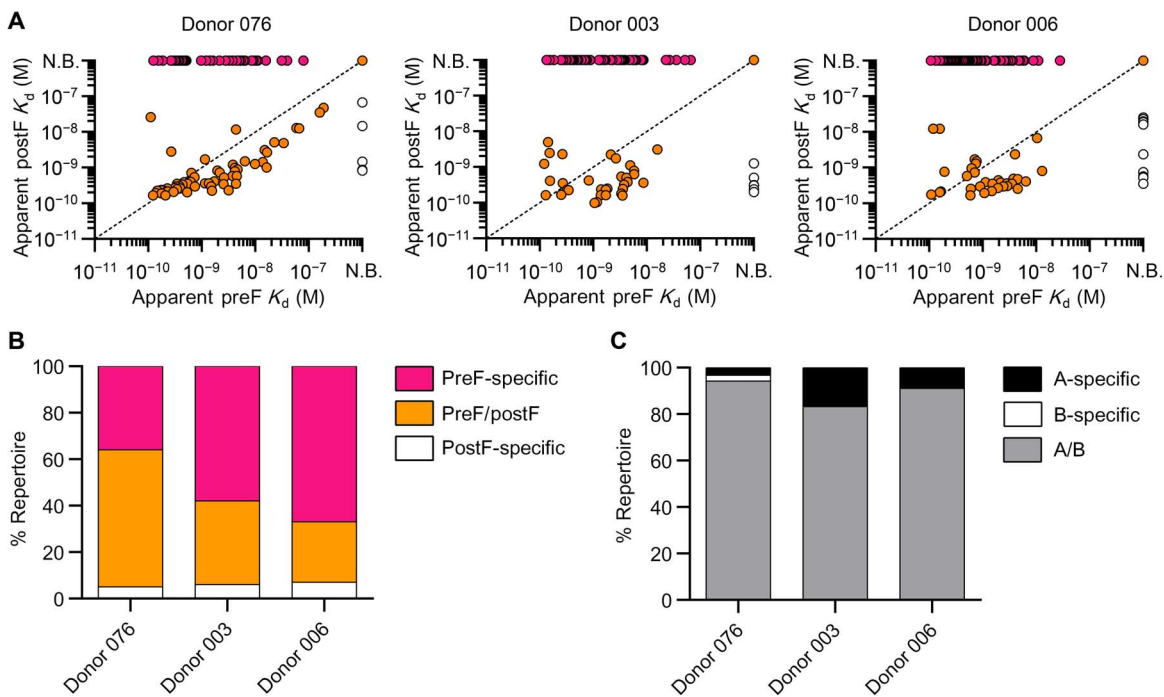


Fig. 2. Antibody preferences for conformational state and subtype of RSV F are similar across three adult donor repertoires. (A) IgG affinities for preF and postF are plotted for each donor. PreF-specific antibodies are colored pink, preF/postF-cross-reactive antibodies are orange, and postF-specific antibodies are white. N.B., nonbinding. (B) Percentage of antibodies within each donor repertoire that are preF-specific, preF/postF-cross-reactive, or postF-specific. (C) Percentage of antibodies within each donor repertoire that bind specifically to RSV F derived from subtype A (black), subtype B (white), or both subtypes A and B (gray).

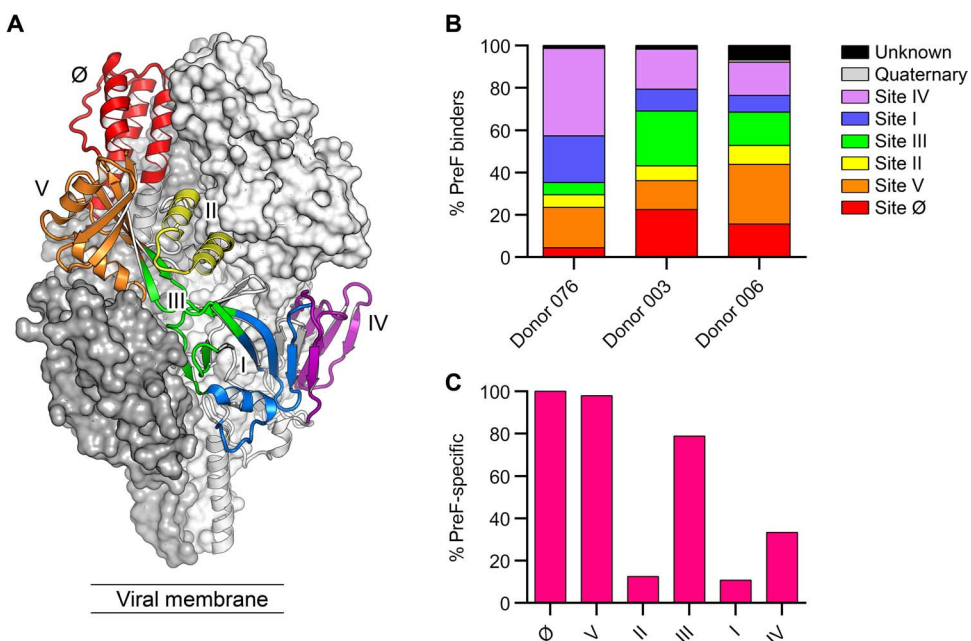


Fig. 3. Antibodies isolated from adult donors recognize six antigenic sites spanning the surface of preF. (A) Structure of RSV preF with one protomer shown as a ribbon colored by antigenic site. (B) Percentage of antibodies targeting each antigenic site within each donor repertoire. The antigenic sites recognized by 215 antibodies with higher than 2 nM affinity for preF were mapped using a combination of antibody binning and patch variant mutational analysis. (C) Percentage of preF-specific antibodies targeting each antigenic site.

22% of antibodies from each donor recognized site Ø and between 6 and 26% recognized site III. A relatively large proportion of antibodies from each donor (14 to 28%) recognized the previously undescribed site V

preF to postF. In summary, the epitope mapping data show that the large majority of isolated antibodies target six major antigenic sites, about half of which are exclusively present on preF.

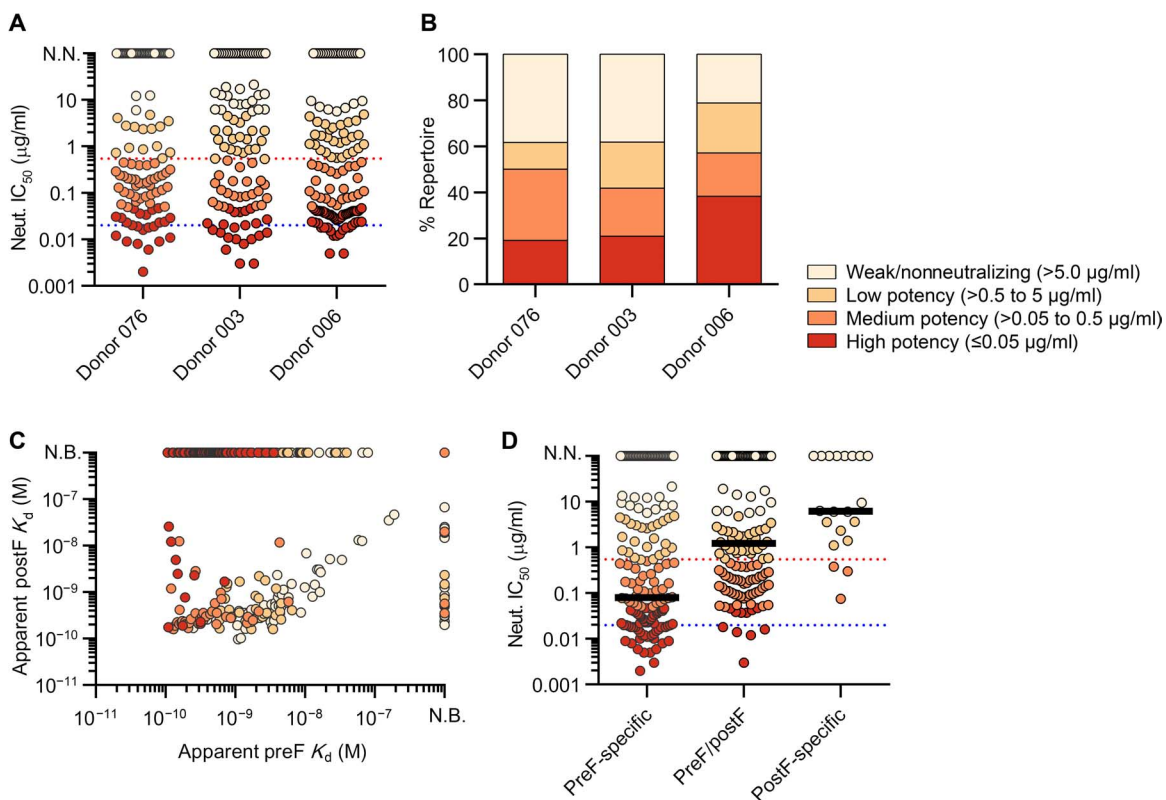


Fig. 4. The majority of potent neutralizing antibodies recognize preF-specific sites. (A) Neutralization IC_{50} values for the antibodies isolated from each donor repertoire. Data points are colored based on neutralization potency. Red and blue dotted lines depict motavizumab and D25 IC_{50} values, respectively. N.N., nonneutralizing. (B) Percentage of neutralizing antibodies in each donor repertoire, grouped by potency. (C) Apparent binding affinities for preF and postF are plotted for each antibody and colored according to neutralization potency. (D) Neutralization IC_{50} values are plotted for preF-specific, postF-specific, and cross-reactive antibodies. Red and blue dotted lines depict motavizumab and D25 IC_{50} values, respectively. Black bar depicts median IC_{50} .

Highly potent neutralizing antibodies target preF-specific epitopes

The 364 IgGs were tested for neutralizing activity against RSV subtypes A and B using a previously described high-throughput neutralization assay (15). For all three donor repertoires, 64 to 80% of the isolated antibodies showed neutralizing activity, and 19 to 38% neutralized with high potency [half maximal inhibitory concentration (IC_{50}) $\leq 0.05 \mu\text{g/ml}$] (Fig. 4, A and B). Several clonally unrelated antibodies were ≥ 5 -fold more potent than D25 and ≥ 100 -fold more potent than palivizumab (Fig. 4A). There was no correlation between neutralization potency and level of SHM ($P = 0.89$, $r = 0.0082$) (fig. S7 and data file S1), suggesting that extensive SHM is not required for potent neutralization of RSV. Consistent with the binding cross-reactivity data, the majority of neutralizing antibodies showed activity against both subtypes A and B (fig. S8).

We next analyzed the relationship between preF- and postF-binding affinity and neutralization potency (Fig. 4C). This analysis revealed that greater than 85% of highly potent antibodies ($IC_{50} \leq 0.05 \mu\text{g/ml}$) were specific for preF (fig. S9). Furthermore, preF-specific antibodies were >10 -fold more potent than preF and postF cross-reactive antibodies and about 80-fold more potent than antibodies that specifically recognized postF (Fig. 4D). There was a positive correlation between preF binding and neutralization ($P < 0.001$, $r = 0.24$), and the apparent preF equilibrium dissociation constants (K_d values) generally corresponded well with the neutralization IC_{50} values (Fig. 5A).

In contrast, there was no correlation between postF binding and neutralization ($P = 0.44$, $r = -0.07$) (Fig. 5B). In addition, relatively few antibodies neutralized with IC_{50} values lower than 100 pM, which is consistent with the previously proposed ceiling to affinity maturation (47, 48).

We next analyzed the relationship between neutralization potency and antigenic site (Fig. 5C). More than 60% of the highly potent neutralizing antibodies targeted antigenic sites Ø and V, which represent two of the three preF specific sites. In contrast, antibodies targeting sites III and IV showed a wide range of neutralization potencies, and antibodies targeting sites I and II were generally moderate to nonneutralizing. Similar results were obtained for subtype B viruses (fig. S10). A subset of site IV-directed antibodies neutralized with substantially lower potency than would be expected based on preF binding affinity (Fig. 5A). There are several possible explanations for this observation, including differences in (i) the ability of antibodies to access these sites on the crowded surface of the virion, (ii) the sensitivity of different sites to the antibody angle of approach, and (iii) the mechanisms of neutralization for preF-specific antibodies compared with antibodies that are reactive with both preF and postF.

Several antibodies cross-neutralize RSV and HMPV

Given that the RSV and human metapneumovirus (HMPV) mature F protein ectodomains share about 38% amino acid identity, and certain RSV F-specific antibodies cross-neutralize HMPV (17, 49), we next tested the antibodies in our panel for neutralizing activity against

HMPV. Of the 364 antibodies tested, nine neutralized HMPV and two showed highly potent activity against both HMPV and RSV (Table 1). Sequence analysis revealed that the nine antibodies comprise five clonal

families, which do not show convergent VH germline gene usage, CDRH3 lengths, or somatic mutations (data file S3). Nearly all the cross-neutralizing antibodies bound exclusively to preF and competed with MPE8 (antigenic site III) (Table 1). This result was not unexpected because MPE8 has been previously shown to cross-neutralize four pneumoviruses, including RSV and HMPV (17). Although HMPV F was not used for B cell sorting, all three donor repertoires contained antibodies that cross-neutralized HMPV, suggesting that highly conserved epitopes are relatively immunogenic in the context of natural RSV and HMPV infection.

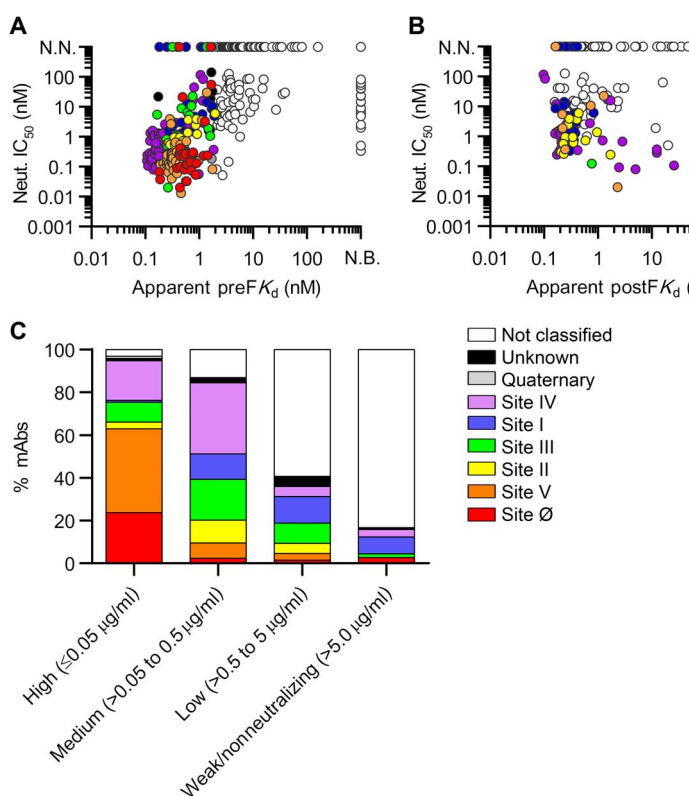


Fig. 5. The most potent neutralizing antibodies bind with high affinity to preF and recognize antigenic sites Ø and V. (A) Neutralization IC₅₀ is plotted against apparent preF K_d and colored according to antigenic site. (B) Neutralization IC₅₀ is plotted against apparent postF K_d and colored by antigenic site. (C) Antibodies are grouped according to neutralization potency and colored by antigenic site.

DISCUSSION

An in-depth understanding of the human antibody response to RSV infection will aid the development and evaluation of RSV vaccine candidates. Although previous studies have coarsely mapped the epitopes targeted by RSV-specific neutralizing antibodies in human sera (4, 8), the specificities and functional properties of antibodies induced by natural RSV infection have remained largely undefined. Here, we have used preF- and postF-stabilized proteins (11, 15), a high-throughput antibody isolation platform, and a structure-guided collection of preF mutants to clonally dissect the human memory B cell response to RSV F in three naturally infected adult donors.

In the repertoires analyzed, the ratio of preF-specific antibodies to those that recognize both preF and postF varied slightly among the three donors, with an average ratio of about 1:1. These values are somewhat lower than those reported for human sera, which showed that about 70% of anti-F serum binding is specific for preF (8). This discrepancy may be the result of differences between the levels of individual antibodies in serum, differences in the B cell phenotypes achieved for a particular specificity, or variation between donors. Despite these minor differences,

Table 1. A subset of anti-RSV F antibodies cross-neutralize HMPV. N.B., nonbinder.

Name	HMPV-A1 IC ₅₀ (µg/ml)	RSV-A2 IC ₅₀ (µg/ml)	Prefusion RSV F K _d (M)	Postfusion RSV F K _d (M)	RSV F binding site
ADI-14448	0.05	0.04	3.8×10^{-10}	N.B.	III
ADI-15614	0.22	0.03	4.1×10^{-10}	N.B.	III
ADI-14441	37.8	>25	8.6×10^{-9}	N.B.	III*
ADI-14501	31.4	12.4	1.6×10^{-8}	N.B.	III*
ADI-15657	11.9	>25	5.7×10^{-9}	N.B.	III*
ADI-15665	13.5	12.7	8.3×10^{-9}	N.B.	III*
ADI-15647	20.3	>25	7.8×10^{-9}	N.B.	III*
ADI-15623	0.37	0.05	2.1×10^{-9}	N.B.	III*
ADI-18992	6.1	2.5	7.6×10^{-10}	1.5×10^{-9}	IV*
MPE8 control	0.07	0.04	—	—	—

*Binding site assignment based on competition only.

the results of both studies suggest that preF-specific epitopes and epitopes shared by preF and postF are immunogenic during natural RSV infection, whereas the unique surfaces on postF are substantially less immunogenic.

Our repertoire analysis reveals that the large majority of RSV F-specific antibodies target six major antigenic sites on prefusion RSV F: Ø, I, II, III, IV, and V. We defined these sites based on previously determined structures, resistance mutations, and secondary structure of the preF protein. It is important to note that the nomenclature for describing RSV F antigenic sites has evolved over time (6, 50–56), and previous mapping efforts were based on the postfusion conformation of F and did not include surfaces present exclusively on preF. The crystal structure of preF has provided critical information about F structure and function as well as new reagents to map antibody binding sites on the unique surfaces of preF and surfaces shared with postF. We therefore propose an update to the nomenclature system for antigenic sites on RSV F, building on previous information but now including structurally defined regions of preF. To a first approximation, each antibody can be assigned primarily to one of these sites. However, it is likely that antibody epitopes cover the entire surface of F and that there are antibodies that bind two or more adjacent antigenic sites within a protomer and quaternary antibodies that bind across protomers. Thus, the antigenic site nomenclature is not precise enough to describe the entire spectrum of RSV F-specific antibodies but should be considered as a rationally defined three-dimensional guide to the major antigenic sites of preF.

The results show that the most potently neutralizing antibodies target antigenic sites Ø and V, both of which are located near the apex of the preF trimer. These findings are consistent with the results obtained from human sera mapping, which determined that the majority of neutralizing activity can be removed by preincubation with preF (4, 8) and that preF-specific sites other than site Ø make up a considerable fraction of preF-specific neutralizing antibodies (8). Although antigenic site Ø has been shown to be a target of potently neutralizing antibodies (8, 10), the interaction of antibodies with site V is less well understood. We found that the majority of site V-directed antibodies share several convergent sequence features, suggesting that it may be possible to rapidly detect these types of antibodies in human samples using high-throughput sequencing technology (57). This may prove to be particularly useful for profiling antibody responses to RSV vaccine candidates that aim to preserve the apex of the preF trimer.

A limitation of our repertoire analysis is the relatively small number of donors studied. We chose to isolate a large number of mAbs from each donor, rather than to include a large number of donors with limited numbers of antibodies isolated from each. As a result, intradonor comparisons can be made with high certainty, but interdonor comparisons are less robust. However, the high degree of similarity among the three donor repertoires, combined with the overall agreement of our findings with those of the sera analysis published previously (8), suggests that the antibody repertoires analyzed here are likely representative of naturally infected adult donors.

This extensive panel of antibodies provides new opportunities for passive prophylaxis. More than 30 of these antibodies neutralize RSV more potently than does D25, which served as the basis for MEDI8897—an optimized mAb that is currently in clinical trials for the prevention of RSV in young, at-risk children (58). Additionally, we have isolated several antibodies that cross-neutralize HMPV, including one that neutralizes RSV with a potency comparable to that of D25. The identification of a cross-neutralizing antibody with potency equivalent to that of D25 sug-

gests that cross-neutralization of HMPV does not necessarily occur at the expense of potent RSV neutralization.

Although passive prophylaxis with highly potent antibodies may substantially reduce the RSV disease burden in select populations, an effective vaccine would produce the greatest benefit at the lowest cost. The development of an RSV vaccine has presented a number of unique challenges, and selection of the optimal vaccination strategy will be of the utmost importance. The in-depth analysis of the human antibody response to natural RSV infection presented here provides insights into the development of such a vaccine. Our results suggest that immunization of pre-immune individuals with preF immunogens will likely boost neutralizing responses, whereas the use of postF immunogens would be expected to expand B cell clones with moderate or weak neutralizing activity. Similarly, immunization of RSV-naïve infants with preF immunogens would be expected to activate naïve B cells targeting epitopes associated with substantially more potent neutralizing activity compared with postF immunogens. In addition, the ideal RSV vaccine should preserve antigenic sites Ø and V because these sites are targeted by the most highly potent antibodies elicited in response to natural RSV infection. Last, the reagents described here provide a useful set of tools for the evaluation of clinical trials, which will be critical for selecting the optimal RSV vaccination strategy from the many currently under investigation (59).

MATERIALS AND METHODS

Study design

We initiated this study to gain an in-depth understanding of the antibody response to RSV F in naturally infected adult donors. To profile the antibody response to RSV F, we obtained peripheral blood mononuclear cells (PBMCs) from three healthy adult donors that were between 20 and 35 years of age and generated mAbs from RSV F-reactive B cells. Three donors were included in this study because this was the largest number of donors for which large numbers of antibodies could be practically cloned and characterized. Two independent experiments were performed for affinity measurements and antibody competition assays, and the results shown are derived from a single-representative experiment. For neutralization assays and patch assignments, the results are derived from a single experiment with eight serial dilutions. All samples for this study were collected with informed consent of volunteers. This study was unblinded and not randomized.

Generation of RSV F sorting probes

The soluble pre- and postfusion probes were based on the DS-Cav1 and RSV F ΔFP constructs that we previously crystallized and determined to be in the pre- and postfusion conformations, respectively (11, 15). To increase the avidity of our probes and to uniformly orient the RSV F proteins, we coupled the trimeric RSV F proteins to tetrameric streptavidin through biotinylation of a C-terminal AviTag. For each probe, both a C-terminal 6×His-AviTag version and a C-terminal Strep-tag II version were cotransfected into FreeStyle 293-F cells. The secreted proteins were purified first over Ni-nitrilotriacetic acid (NTA) resin to remove trimers lacking the 6×His-AviTag. The elution from the Ni-NTA purification was then purified over Strep-Tactin resin to remove trimers lacking the Strep-tag II. Because of the low avidity of a single Strep-tag II for the Strep-Tactin resin, additional washing steps could remove trimers containing a single Strep-tag II. This resulted in the purification of trimers containing two Strep-tag II monomers and

one 6×His-AviTag monomer. The presence of a single AviTag per trimer greatly reduces the aggregation or “daisy chaining” that occurs when trimeric proteins containing three AviTags are incubated with tetrameric streptavidin. RSV F trimers were biotinylated using biotin ligase BirA according to the manufacturer’s instructions (Avidity LLC). Biotinylated proteins were separated from excess biotin by size-exclusion chromatography on a Superdex 200 column (GE Healthcare). Quantitation of the number of biotin moieties per RSV F trimer was performed using the Quant*Tag Biotin Quantitation Kit per the manufacturer’s instructions (Vector Laboratories). Dual-labeled RSV F tetramers were generated by incubating the individual AviTagged RSV F proteins with premium-grade phycoerythrin (PE)-labeled streptavidin (Molecular Probes) or premium-grade allophycocyanin-labeled streptavidin for at least 20 min on ice at a molar ratio of 4:1. Tetramers were prepared fresh for each experiment.

Single B cell sorting

PBMCs were stained using anti-human IgG (BV605), IgA [fluorescein isothiocyanate (FITC)], CD27 (BV421), CD8 [peridinin chlorophyll protein (PerCP)-Cy5.5], CD14 (PerCP-Cy5.5), CD19 (PECy7), CD20 (PECy7), and a mixture of dual-labeled RSV F pre- and postfusion tetramers (50 nM each). Single cells were sorted on BD FACSAria II into 96-well PCR plates (Bio-Rad) containing 20 μ l per well of lysis buffer [5 μ l of 5× first-strand complementary DNA buffer (Invitrogen), 0.25 μ l of RNaseOUT (Invitrogen), 1.25 μ l of dithiothreitol (Invitrogen), 0.625 μ l of NP-40 (New England Biolabs), and 12.6 μ l of distilled water]. Plates were immediately frozen on dry ice before storage at –80°C.

Amplification and cloning of antibody variable genes

Single B cell PCR was performed as described previously (22). Briefly, IgH, Ig λ , and Ig κ variable genes were amplified by reverse transcription PCR and nested PCRs using cocktails of IgG- and IgA-specific primers (22). The primers used in the second round of PCR contained 40 base pairs of 5’ and 3’ homology to the digested expression vectors to allow for cloning by homologous recombination into *S. cerevisiae* (40). PCR products were cloned into *S. cerevisiae* using the lithium acetate method for chemical transformation (41). Each transformation reaction contained 20 μ l of unpurified heavy chain and light chain PCR product and 200 ng of cut heavy and light chain plasmids. After transformation, individual yeast colonies were picked for sequencing and characterization.

Expression and purification of IgGs and Fab fragments

Anti-RSV F IgGs were expressed in *S. cerevisiae* cultures grown in 24-well plates, as described previously (23). Fab fragments used for competition assays were generated by digesting the IgGs with papain for 2 hours at 30°C. The digestion was terminated by the addition of iodoacetamide, and the Fab and Fc mixtures were passed over protein A agarose to remove Fc fragments and undigested IgG. The flow-through of the protein A resin was then passed over CaptureSelect IgG-CH1 affinity resin (Thermo Fisher Scientific) and eluted with 200 mM acetic acid and 50 mM NaCl (pH 3.5) into one-eighth volume of 2 M Hepes (pH 8.0). Fab fragments were then buffer-exchanged into phosphate-buffered saline (PBS; pH 7.0).

Biolayer interferometry binding analysis

IgG binding to DS-Cav1 and F ΔFP was determined by biolayer interferometry (BLI) measurements using a FortéBio Octet HTX instrument (Pall Life Sciences). For high-throughput K_d determination,

IgGs were immobilized on anti-human IgG quantitation biosensors (Pall Life Sciences) and exposed to 100 nM antigen in PBS containing 0.1% bovine serum albumin (BSA) (PBSF) for an association step, followed by a dissociation step in PBSF buffer. Data were analyzed using the FortéBio Data Analysis Software 7. IgG K_d values were calculated for antibodies with BLI responses of >0.1 nm. Antibodies with BLI responses of <0.1 nm were designated as nonbinders. The data were fit to a 1:1 binding model to calculate association and dissociation rate constants, and K_d was calculated using the ratio k_d/k_a .

Antibody competition assays

Antibody competition assays were performed as previously described (23). Antibody competition was measured by the ability of a control anti-RSV F Fab to inhibit binding of yeast surface-expressed anti-RSV F IgGs to either DS-Cav1 or F ΔFP. Biotinylated DS-Cav1 or F ΔFP (50 nM) was preincubated with 1 μ M competitor Fab for 30 min at room temperature and then added to a suspension of yeast expressing anti-RSV F IgG. Unbound antigen was removed by washing with PBSF. After washing, bound antigen was detected using streptavidin Alexa Fluor 633 at a 1:500 dilution (Life Technologies) and analyzed by flow cytometry using FACSCanto II (BD Biosciences). The level of competition was assessed by measuring the fold reduction in antigen binding in the presence of competitor Fab relative to an antigen-only control. Antibodies were considered competitors when a greater than fivefold reduction was observed in the presence of control Fab relative to an antigen-only control.

Expression, purification, and biotinylation of preF patch variants

A panel of nine preF variants, each containing a patch of two to four mutations, was designed based on the structure of preF (10). For known antigenic sites, including those recognized by motavizumab, 101F, D25, AM14, and MPE8, the patches contained substitutions associated with viral escape or decreased antibody binding. Residues with high conservation across 184 subtype A, subtype B, and bovine RSV F sequences were avoided, where possible, to minimize the likelihood of disrupting protein structure. The mutations present in each patch variant are shown in fig. S4. Mutations for each patch variant were cloned into the DS-Cav1 construct with a C-terminal AviTag for site-specific biotinylation. Proteins were secreted from FreeStyle 293-F cells, purified over Ni-NTA resin, and biotinylated using biotin ligase BirA according to the manufacturer’s instructions (Avidity LLC). Biotinylated proteins were separated from excess biotin by size-exclusion chromatography on a Superdex 200 column (GE Healthcare). A deglycosylated variant was produced by expressing DS-Cav1 in the presence of 1 μ M kifunensine and digesting with 10% (w/w) EndoH before biotinylation.

Luminex assay for patch variant binding

Binding of isolated antibodies to the patch variants was determined using a high-throughput Luminex assay. Each biotinylated variant and a DS-Cav1 control were coupled to avidin-coated MagPlex beads (Bio-Rad), each with a bead identification number reflecting a unique ratio of red and infrared dyes embedded within the bead. The coupled beads were then mixed with a sixfold serial dilution of each antibody, ranging from 400 nM to 1.4 pM, in a 384-well plate. Beads were washed using a magnetic microplate washer (BioTek) before incubation with a PE-conjugated mouse anti-human IgG Fc secondary antibody (SouthernBiotech). Beads were classified, and binding of PE was measured using a FLEXMAP 3D flow cytometer (Luminex).

RSV neutralization assays

Viral stocks were prepared and maintained as previously described (60). Recombinant mKate-RSV expressing prototypic subtype A (strain A2) and subtype B (18537) F genes and the Katushka fluorescent protein were constructed as reported by Hotard *et al.* (61). HEp-2 cells were maintained in Eagle's minimum essential medium containing 10% fetal bovine serum supplemented with glutamine, penicillin, and streptomycin. Antibody neutralization was measured by a fluorescence plate reader neutralization assay (15). A 30-μl solution of culture medium containing 2.4 × 10⁴ HEp-2 cells was seeded in 384-well black optical bottom plates (Nunc, Thermo Fisher Scientific). IgG samples were serially diluted fourfold from 1:10 to 1:163,840, and an equal volume of recombinant mKate-RSV A2 was added. Samples were mixed and incubated at 37°C for 1 hour. After incubation, a 50-μl mixture of sample and virus was added to cells in 384-well plates and incubated at 37°C for 22 to 24 hours. The assay plate was then measured for fluorescence intensity in a microplate reader at an excitation of 588 nm and an emission of 635 nm (SpectraMax Paradigm, Molecular Devices). IC₅₀ of neutralization for each sample was calculated by curve fitting using Prism (GraphPad Software Inc.).

HMPV neutralization assays

Predetermined amounts of recombinant green fluorescent protein (GFP)-expressing HMPV (NL1/00, A1 sublineage, a gift from B. van den Hoogen and R. Fouchier, Rotterdam, Netherlands) were mixed with serial dilutions of mAbs before they were added to Vero-118 cells growing in 96-well plates with Dulbecco's modified Eagle's medium supplemented with 10% fetal calf serum. Thirty-six hours later, the medium was removed, PBS was added, and the amount of GFP per well was measured with a Tecan M200 microplate reader. Fluorescence values were represented as percent of a virus control without antibody.

Polyreactivity assay

Antibody polyreactivity was assessed using a previously described high-throughput assay that measures binding to solubilized Chinese hamster ovary cell membrane preparations (SMPs) (43). Briefly, 2 million IgG-presenting yeast were transferred into a 96-well assay plate and pelleted to remove the supernatant. The pellet was resuspended in 50 μl of 1:10 diluted stock biotinylated SMPs and incubated on ice for 20 min. Cells were then washed twice with ice-cold PBSF, and the cell pellet was resuspended in 50 μl of secondary labeling mix (ExtrAvidin-R-PE, anti-human light chain-FITC, and propidium iodide). The mix was incubated on ice for 20 min, followed by two washes with ice-cold PBSF. Cells were then resuspended in 100 μl of ice-cold PBSF, and the plate was run on a FACSCanto II (BD Biosciences) using a high-throughput sample injector. Flow cytometry data were analyzed for mean fluorescence intensity in the R-PE channel and normalized to proper controls to assess nonspecific binding.

Statistical analyses

In Fig. 5 and fig. S7, statistical significance was determined using Pearson product-moment correlation and Spearman rank correlation analysis, respectively. Antibodies that failed to bind or neutralize were excluded from the statistical analysis because of the inability to accurately calculate midpoint concentrations.

SUPPLEMENTARY MATERIALS

immunology.scienmag.org/cgi/content/full/1/6/eaaj1879/DC1

Fig. S1. Purification of preF and postF sorting probes.

Fig. S2. Representative gating strategy for RSV F-specific B cell sorting.

Fig. S3. Anti-RSV F antibodies lack polyreactivity.

Fig. S4. Generation and validation of preF patch panel mutants.

Fig. S5. Antibody binding affinities for preF and postF.

Fig. S6. Antigenic site V resides between the epitopes recognized by D25, MPE8, and motavizumab.

Fig. S7. Degree of SHM does not correlate with neutralization potency.

Fig. S8. Neutralization of RSV subtype B.

Fig. S9. Neutralizing activities of preF-specific, cross-reactive, and postF-specific antibodies.

Fig. S10. Relationship between subtype B neutralization and epitope.

Table S1. Antigenic sites targeted by prototypic RSV antibodies.

Table S2. Efficiency of binder rescue from B cell sorting.

Table S3. Competition profile of antibodies used in binning experiments.

Data file S1. Binding, neutralization, epitope assignment, limited sequence features, and GenBank accession codes for the isolated antibodies.

Data file S2. Site V-directed antibodies show convergent sequence features.

Data file S3. Antibody variable gene sequences of HMPV cross-neutralizing antibodies.

Reference (62)

REFERENCES AND NOTES

- A. L. Rogovik, B. Carleton, A. Solimano, R. D. Goldman, Palivizumab for the prevention of respiratory syncytial virus infection. *Can. Fam. Physician* **56**, 769–772 (2010).
- B. S. Graham, Biological challenges and technological opportunities for respiratory syncytial virus vaccine development. *Immunol. Rev.* **239**, 149–166 (2011).
- J. R. Groothuis, E. A. F. Simoes, V. G. Hemming, Respiratory syncytial virus (RSV) infection in preterm infants and the protective effects of RSV immune globulin (RSVIG). *Respiratory Syncytial Virus Immune Globulin Study Group. Pediatrics* **95**, 463–467 (1995).
- M. Magro, V. Mas, K. Chappell, M. Vázquez, O. Cano, D. Luque, M. C. Terrón, J. A. Melero, C. Palomo, Neutralizing antibodies against the preactive form of respiratory syncytial virus fusion protein offer unique possibilities for clinical intervention. *Proc. Natl. Acad. Sci. U.S.A.* **109**, 3089–3094 (2012).
- S. Johnson, C. Oliver, G. A. Prince, V. G. Hemming, D. S. Pfarr, S.-C. Wang, M. Dormitzer, J. O'Grady, S. Koenig, J. K. Tamura, R. Woods, G. Bansal, D. Couchenour, E. Tsao, W. C. Hall, J. F. Young, Development of a humanized monoclonal antibody (MEDI-493) with potent in vitro and in vivo activity against respiratory syncytial virus. *J. Infect. Dis.* **176**, 1215–1224 (1997).
- J. A. Beeler, K. van Wyke Coelingh, Neutralization epitopes of the F glycoprotein of respiratory syncytial virus: Effect of mutation upon fusion function. *J. Virol.* **63**, 2941–2950 (1989).
- R. A. Karron, D. A. Buonaguro, A. F. Georgiu, S. S. Whitehead, J. E. Adamus, M. L. Clements-Mann, D. O. Harris, V. B. Randolph, S. A. Udem, B. R. Murphy, M. S. Sidhu, Respiratory syncytial virus (RSV) SH and G proteins are not essential for viral replication in vitro: Clinical evaluation and molecular characterization of a cold-passaged, attenuated RSV subgroup B mutant. *Proc. Natl. Acad. Sci. U.S.A.* **94**, 13961–13966 (1997).
- J. O. Ngwuta, M. Chen, K. Modjarrad, M. G. Joyce, M. Kanekiyo, A. Kumar, H. M. Yassine, S. M. Moin, A. M. Killikelly, G.-Y. Chuang, A. Druz, I. S. Georgiev, E. J. Rundlet, M. Sastry, G. B. E. Stewart-Jones, Y. Yang, B. Zhang, M. C. Nason, C. Capella, M. E. Peebles, J. E. Ledgerwood, J. S. McLellan, P. D. Kwong, B. S. Graham, Prefusion F-specific antibodies determine the magnitude of RSV neutralizing activity in human sera. *Sci. Transl. Med.* **7**, 309ra162 (2015).
- The IMPact-RSV Study Group, Palivizumab, a humanized respiratory syncytial virus monoclonal antibody, reduces hospitalization from respiratory syncytial virus infection in high-risk infants. *Pediatrics* **102** (3 Pt. 1), 531–537 (1998).
- J. S. McLellan, M. Chen, S. Leung, K. W. Graepel, X. Du, Y. Yang, T. Zhou, U. Baxa, E. Yasuda, T. Beaumont, A. Kumar, K. Modjarrad, Z. Zheng, M. Zhao, N. Xia, P. D. Kwong, B. S. Graham, Structure of RSV fusion glycoprotein trimer bound to a prefusion-specific neutralizing antibody. *Science* **340**, 1113–1117 (2013).
- J. S. McLellan, Y. Yang, B. S. Graham, P. D. Kwong, Structure of respiratory syncytial virus fusion glycoprotein in the postfusion conformation reveals preservation of neutralizing epitopes. *J. Virol.* **85**, 7788–7796 (2011).
- K. A. Swanson, E. C. Settembre, C. A. Shaw, A. K. Dey, R. Rappuoli, C. W. Mandl, P. R. Dormitzer, A. Carfi, Structural basis for immunization with postfusion respiratory syncytial virus fusion F glycoprotein (RSV F) to elicit high neutralizing antibody titers. *Proc. Natl. Acad. Sci. U.S.A.* **108**, 9619–9624 (2011).
- L. Liljeroos, M. A. Krzyzaniak, A. Helenius, S. J. Butcher, Architecture of respiratory syncytial virus revealed by electron cryomicroscopy. *Proc. Natl. Acad. Sci. U.S.A.* **110**, 11133–11138 (2013).
- A. Krarup, D. Truan, P. Furmanova-Hollenstein, L. Bogaert, P. Bouchier, I. J. M. Bisschop, M. N. Widjojoatmodjo, R. Zahn, H. Schuitemaker, J. S. McLellan, J. P. M. Langedijk, A highly stable prefusion RSV F vaccine derived from structural analysis of the fusion mechanism. *Nat. Commun.* **6**, 8143 (2015).

15. J. S. McLellan, M. Chen, M. G. Joyce, M. Sastry, G. B. E. Stewart-Jones, Y. Yang, B. Zhang, L. Chen, S. Srivatsan, A. Zheng, T. Zhou, K. W. Graepel, A. Kumar, S. Moin, J. C. Boyington, G.-Y. Chuang, C. Soto, U. Baxa, A. Q. Bakker, H. Spits, T. Beaumont, Z. Zheng, N. Xia, S.-Y. Ko, J.-P. Todd, S. Rao, B. S. Graham, P. D. Kwong, Structure-based design of a fusion glycoprotein vaccine for respiratory syncytial virus. *Science* **342**, 592–598 (2013).
16. M. J. Kwakkenbos, S. A. Diehl, E. Yasuda, A. Q. Bakker, C. M. M. van Geelen, M. V. Lukens, G. M. van Bleek, M. N. Widjojoatmodjo, W. M. J. M. Bogers, H. Mei, A. Radbruch, F. A. Scheeren, H. Spits, T. Beaumont, Generation of stable monoclonal antibody-producing B cell receptor-positive human memory B cells by genetic programming. *Nat. Med.* **16**, 123–128 (2010).
17. D. Corti, S. Bianchi, F. Vanzetta, A. Minola, L. Perez, G. Agatic, B. Guarino, C. Silacci, J. Marcandalli, B. J. Marsland, A. Piralla, E. Percivalle, F. Sallusto, F. Baldanti, A. Lanzavecchia, Cross-neutralization of four paramyxoviruses by a human monoclonal antibody. *Nature* **501**, 439–443 (2013).
18. M. Magro, D. Andreu, P. Gómez-Puertas, J. A. Melero, C. Palomo, Neutralization of human respiratory syncytial virus infectivity by antibodies and low-molecular-weight compounds targeted against the fusion glycoprotein. *J. Virol.* **84**, 7970–7982 (2010).
19. G. Taylor, E. J. Stott, J. Furze, J. Ford, P. Sopp, Protective epitopes on the fusion protein of respiratory syncytial virus recognized by murine and bovine monoclonal antibodies. *J. Gen. Virol.* **73** (Pt. 9), 2217–2223 (1992).
20. L. J. Calder, L. González-Reyes, B. García-Barreno, S. A. Wharton, J. J. Skehel, D. C. Wiley, J. A. Melero, Electron microscopy of the human respiratory syncytial virus fusion protein and complexes that it forms with monoclonal antibodies. *Virology* **271**, 122–131 (2000).
21. M. S. A. Gilman, S. M. Moin, V. Mas, M. Chen, N. K. Patel, K. Kramer, Q. Zhu, S. C. Kabache, A. Kumar, C. Palomo, T. Beaumont, U. Baxa, N. D. Ulbrant, J. A. Melero, B. S. Graham, J. S. McLellan, Characterization of a prefusion-specific antibody that recognizes a quaternary, cleavage-dependent epitope on the RSV fusion glycoprotein. *PLOS Pathog.* **11**, e1005035 (2015).
22. M. G. Joyce, A. K. Wheatley, P. V. Thomas, G.-Y. Chuang, C. Soto, R. T. Bailer, A. Druz, I. S. Georgiev, R. A. Gillespie, M. Kanekiyo, W.-P. Kong, K. Leung, S. N. Narpaia, M. S. Prabhakaran, E. S. Yang, B. Zhang, Y. Zhang, M. Asokan, J. C. Boyington, T. Bylund, S. Darko, C. R. Lees, A. Ransier, C.-H. Shen, L. Wang, J. R. Whittle, X. Wu, H. M. Yassine, C. Santos, Y. Matsuoka, Y. Tsbytovskiy, U. Baxa; NISC Comparative Sequencing Program, J. C. Mullikin, K. Subbarao, D. C. Douek, B. S. Graham, R. A. Koup, J. E. Ledgerwood, M. Roederer, L. Shapiro, P. D. Kwong, J. R. Mascola, A. B. McDermott, Vaccine-induced antibodies that neutralize group 1 and group 2 influenza A viruses. *Cell* **166**, 609–623 (2016).
23. J. Truck, M. N. Ramasamy, J. D. Galson, R. Rance, J. Parkhill, G. Lunter, A. J. Pollard, D. F. Kelly, Identification of antigen-specific B cell receptor sequences using public repertoire analysis. *J. Immunol.* **194**, 252–261 (2015).
24. P. Parameswaran, Y. Liu, K. M. Roskin, K. K. L. Jackson, V. P. Dixit, J.-Y. Lee, K. L. Artiles, S. Zompi, M. J. Vargas, B. B. Simen, B. Hanczaruk, K. R. McGowan, M. A. Tariq, N. Pourmand, D. Koller, A. Balmaseda, S. D. Boyd, E. Harris, A. Z. Fire, Convergent antibody signatures in human dengue. *Cell Host Microbe* **13**, 691–700 (2013).
25. K. J. L. Jackson, Y. Liu, K. M. Roskin, J. Glanville, R. A. Hoh, K. Seo, E. L. Marshall, T. C. Gurley, M. A. Moody, B. F. Haynes, E. B. Walter, H.-X. Liao, R. A. Albrecht, A. García-Sastre, J. Chaparro-Riggers, A. Rajpal, J. Pons, B. B. Simen, B. Hanczaruk, C. L. Dekker, J. Laserson, D. Koller, M. M. Davis, A. Z. Fire, S. D. Boyd, Human responses to influenza vaccination show seroconversion signatures and convergent antibody rearrangements. *Cell Host Microbe* **16**, 105–114 (2014).
26. F. W. Henderson, A. M. Collier, W. A. Clyde Jr., F. W. Denny, Respiratory-syncytial-virus infections, reinfections and immunity—A prospective, longitudinal study in young children. *N. Engl. J. Med.* **300**, 530–534 (1979).
27. M. A. Moody, B. F. Haynes, Antigen-specific B cell detection reagents: Use and quality control. *Cytometry A* **73A**, 1086–1092 (2008).
28. M. S. Habibi, A. Jozwik, S. Makris, J. Dunning, A. Paras, J. P. DeVincenzo, C. A. M. de Haan, J. Wrammert, P. J. M. Openshaw, C. Chiu; Mechanisms of Severe Acute Influenza Consortium Investigators, Impaired antibody-mediated protection and defective IgA B-cell memory in experimental infection of adults with respiratory syncytial virus. *Am. J. Respir. Crit. Care Med.* **191**, 1040–1049 (2015).
29. T. Tiller, E. Meffre, S. Yurasov, M. Tsuji, M. C. Nussenzweig, H. Wardemann, Efficient generation of monoclonal antibodies from single human B cells by single cell RT-PCR and expression vector cloning. *J. Immunol. Methods* **329**, 112–124 (2008).
30. Z. A. Bornholdt, H. L. Turner, C. D. Murin, W. Li, D. Sok, C. A. Souders, A. E. Piper, A. Goff, J. D. Shamblin, S. E. Wollen, T. R. Sprague, M. L. Fusco, K. B. J. Pommert, L. A. Cavacini, H. L. Smith, M. Klempner, K. A. Reimann, E. Krauland, T. U. Gerngross, K. D. Wittrup, E. O. Saphire, D. R. Burton, P. J. Glass, A. B. Ward, L. M. Walker, Isolation of potent neutralizing antibodies from a survivor of the 2014 Ebola virus outbreak. *Science* **351**, 1078–1083 (2016).
31. J. F. Scheid, H. Mouquet, N. Feldhahn, M. S. Seaman, K. Velinzon, J. Pietzsch, R. G. Ott, R. M. Anthony, H. Zebroski, A. Hurley, A. Phogat, B. Chakrabarti, Y. Li, M. Connors, F. Pereyra, B. D. Walker, H. Wardemann, D. Ho, R. T. Wyatt, J. R. Mascola, J. V. Ravetch, M. C. Nussenzweig, Broad diversity of neutralizing antibodies isolated from memory B cells in HIV-infected individuals. *Nature* **458**, 636–640 (2009).
32. J. Wrammert, K. Smith, J. Miller, W. A. Langley, K. Kokko, C. Larsen, N.-Y. Zheng, I. Mays, L. Garman, C. Helms, J. James, G. M. Air, J. D. Capra, R. Ahmed, P. C. Wilson, Rapid cloning of high-affinity human monoclonal antibodies against influenza virus. *Nature* **453**, 667–671 (2008).
33. S. D. Boyd, B. A. Gaëta, K. J. Jackson, A. Z. Fire, E. L. Marshall, J. D. Merker, J. M. Maniar, L. N. Zhang, B. Sahaf, C. D. Jones, B. B. Simen, B. Hanczaruk, K. D. Nguyen, K. C. Nadeau, M. Egholm, D. B. Miklos, J. L. Zehnder, A. M. Collins, Individual variation in the germline Ig gene repertoire inferred from variable region gene rearrangements. *J. Immunol.* **184**, 6986–6992 (2010).
34. J. Sui, W. C. Hwang, S. Perez, G. Wei, D. Aird, L.-m. Chen, E. Santelli, B. Stec, G. Cadwell, M. Ali, H. Wan, A. Murakami, A. Yammanuru, T. Han, N. J. Cox, L. A. Bankston, R. O. Donis, R. C. Liddington, W. A. Marasco, Structural and functional bases for broad-spectrum neutralization of avian and human influenza A viruses. *Nat. Struct. Mol. Biol.* **16**, 265–273 (2009).
35. C.-c. Huang, M. Venturi, S. Majeed, M. J. Moore, S. Phogat, M.-Y. Zhang, D. S. Dimitrov, W. A. Hendrickson, J. Robinson, J. Sodroski, R. Wyatt, H. Choe, M. Farzan, P. D. Kwong, Structural basis of tyrosine sulfation and V_H -gene usage in antibodies that recognize the HIV type 1 coreceptor-binding site on gp120. *Proc. Natl. Acad. Sci. U.S.A.* **101**, 2706–2711 (2004).
36. C. H. Chan, K. G. Hadlock, S. K. H. Foung, S. Levy, V_H -169 gene is preferentially used by hepatitis C virus-associated B cell lymphomas and by normal B cells responding to the E2 viral antigen. *Blood* **97**, 1023–1026 (2001).
37. E. E. Godoy-Lozano, J. Téllez-Sosa, G. Sánchez-González, H. Sámano-Sánchez, A. Aguilar-Salgado, A. Salinas-Rodríguez, B. Cortina-Ceballos, H. Vivanco-Cid, K. Hernández-Flores, J. M. Pfaff, K. M. Kahle, B. J. Doranz, R. E. Gómez-Barreto, H. Valdovinos-Torres, I. López-Martínez, M. H. Rodríguez, J. Martínez-Barnetche, Lower IgG somatic hypermutation rates during acute dengue virus infection is compatible with a germinal center-independent B cell response. *Genome Med.* **8**, 23 (2016).
38. J. Wrammert, D. Koutsonanos, G.-M. Li, S. Edupuganti, J. Sui, M. Morrissey, M. McCausland, I. Skountzou, M. Hornig, W. I. Lipkin, A. Mehta, B. Razavi, C. Del Rio, N.-Y. Zheng, J.-H. Lee, M. Huang, Z. Ali, K. Kaur, S. Andrews, R. R. Amara, Y. Wang, S. R. Das, C. D. O'Donnell, J. W. Yewdell, K. Subbarao, W. A. Marasco, M. J. Mulligan, R. Compans, R. Ahmed, P. C. Wilson, Broadly cross-reactive antibodies dominate the human B cell response against 2009 pandemic H1N1 influenza virus infection. *J. Exp. Med.* **208**, 181–193 (2011).
39. S. F. Andrews, Y. Huang, K. Kaur, L. I. Popova, I. Y. Ho, N. T. Pauli, C. J. Henry Dunand, W. M. Taylor, S. Lim, M. Huang, X. Qu, J.-H. Lee, M. Salgado-Ferrer, F. Krammer, P. Palese, J. Wrammert, R. Ahmed, P. C. Wilson, Immune history profoundly affects broadly protective B cell responses to influenza. *Sci. Transl. Med.* **7**, 316ra192 (2015).
40. M. Liu, G. Yang, K. Wiehe, N. I. Nicely, N. A. Vandergrift, W. Rountree, M. Bonsignori, S. M. Alam, J. Gao, B. F. Haynes, G. Kelsoe, Polyreactivity and autoreactivity among HIV-1 antibodies. *J. Virol.* **89**, 784–798 (2015).
41. H. Mouquet, J. F. Scheid, M. J. Zoller, M. Krosgaard, R. G. Ott, S. Shukair, M. N. Artyomov, J. Pietzsch, M. Connors, F. Pereyra, B. D. Walker, D. Ho, P. C. Wilson, M. S. Seaman, H. N. Eisen, A. K. Chakrabarty, T. J. Hope, J. V. Ravetch, H. Wardemann, M. C. Nussenzweig, Polyreactivity increases the apparent affinity of anti-HIV antibodies by heterologation. *Nature* **467**, 591–595 (2010).
42. R. L. Kelly, T. Sun, T. Jain, I. Caffry, Y. Yu, Y. Cao, H. Lynaugh, M. Brown, M. Vásquez, K. D. Wittrup, Y. Xu, High throughput cross-interaction measures for human IgG1 antibodies correlate with clearance rates in mice. *MAbs* **7**, 770–777 (2015).
43. Y. Xu, W. Roach, T. Sun, T. Jain, B. Prinz, T.-Y. Yu, J. Torrey, J. Thomas, P. Bobrowicz, M. Vásquez, K. D. Wittrup, E. Krauland, Addressing polyclarity of antibodies selected from an in vitro yeast presentation system: A FACS-based, high-throughput selection and analytical tool. *Protein Eng. Des. Sel.* **26**, 663–670 (2013).
44. D. R. Bowley, A. F. Labrijn, M. B. Zwick, D. R. Burton, Antigen selection from an HIV-1 immune antibody library displayed on yeast yields many novel antibodies compared to selection from the same library displayed on phage. *Protein Eng. Des. Sel.* **20**, 81–90 (2007).
45. H. Wu, D. S. Pfarr, S. Johnson, Y. A. Brewah, R. M. Woods, N. K. Patel, W. I. White, J. F. Young, P. A. Kiener, Development of motavizumab, an ultra-potent antibody for the prevention of respiratory syncytial virus infection in the upper and lower respiratory tract. *J. Mol. Biol.* **368**, 652–665 (2007).
46. J. S. McLellan, M. Chen, J.-S. Chang, Y. Yang, A. Kim, B. S. Graham, P. D. Kwong, Structure of a major antigenic site on the respiratory syncytial virus fusion glycoprotein in complex with neutralizing antibody 10F. *J. Virol.* **84**, 12236–12244 (2010).
47. J. Foote, H. N. Eisen, Kinetic and affinity limits on antibodies produced during immune responses. *Proc. Natl. Acad. Sci. U.S.A.* **92**, 1254–1256 (1995).
48. F. D. Batista, M. S. Neuberger, Affinity dependence of the B cell response to antigen: A threshold, a ceiling, and the importance of off-rate. *Immunity* **8**, 751–759 (1998).

49. J. E. Schuster, R. G. Cox, A. K. Hastings, K. L. Boyd, J. Wadia, Z. Chen, D. R. Burton, R. A. Williamson, J. V. Williams, A broadly neutralizing human monoclonal antibody exhibits *in vivo* efficacy against both human metapneumovirus and respiratory syncytial virus. *J. Infect. Dis.* **211**, 216–225 (2015).
50. B. F. Fernie, P. J. Cote Jr., J. L. Gerin, Classification of hybridomas to respiratory syncytial virus glycoproteins. *Proc. Soc. Exp. Biol. Med.* **171**, 266–271 (1982).
51. P. J. Cote Jr., B. F. Fernie, E. C. Ford, J. W.-K. Shih, J. L. Gerin, Monoclonal antibodies to respiratory syncytial virus: Detection of virus neutralization and other antigen-antibody systems using infected human and murine cells. *J. Virol. Methods* **3**, 137–147 (1981).
52. E. E. Walsh, J. Hruska, Monoclonal antibodies to respiratory syncytial virus proteins: Identification of the fusion protein. *J. Virol.* **47**, 171–177 (1983).
53. L. J. Anderson, P. Bingham, J. C. Hierholzer, Neutralization of respiratory syncytial virus by individual and mixtures of F and G protein monoclonal antibodies. *J. Virol.* **62**, 4232–4238 (1988).
54. G. E. Scopes, P. J. Watt, P. R. Lambden, Identification of a linear epitope on the fusion glycoprotein of respiratory syncytial virus. *J. Gen. Virol.* **71** (Pt. 1), 53–59 (1990).
55. J. Arbiza, G. Taylor, J. A. López, J. Furze, S. Wyld, P. Whyte, E. J. Stott, G. Wertz, W. Sullender, M. Trudel, J. A. Melero, Characterization of two antigenic sites recognized by neutralizing monoclonal antibodies directed against the fusion glycoprotein of human respiratory syncytial virus. *J. Gen. Virol.* **73** (Pt. 9), 2225–2234 (1992).
56. J. A. López, R. Bustos, C. Örvell, M. Berois, J. Arbiza, B. García-Barreno, J. A. Melero, Antigenic structure of human respiratory syncytial virus fusion glycoprotein. *J. Virol.* **72**, 6922–6928 (1998).
57. B. J. DeKosky, T. Kojima, A. Rodin, W. Charab, G. C. Ippolito, A. D. Ellington, G. Georgiou, In-depth determination and analysis of the human paired heavy- and light-chain antibody repertoire. *Nat. Med.* **21**, 86–91 (2015).
58. U.S. National Library of Medicine (NCT02290340), <https://clinicaltrials.gov/>.
59. PATH, *RSV Vaccine and mAb Snapshot*; http://sites.path.org/vaccinedevelopment/files/2016/07/RSV-snapshot-July_13_2016.pdf.
60. B. S. Graham, M. D. Perkins, P. F. Wright, D. T. Karzon, Primary respiratory syncytial virus infection in mice. *J. Med. Virol.* **26**, 153–162 (1988).
61. A. L. Hotard, F. Y. Shaikh, S. Lee, D. Yan, M. N. Teng, R. K. Plemper, J. E. Crowe Jr., M. L. Moore, A stabilized respiratory syncytial virus reverse genetics system amenable to recombination-mediated mutagenesis. *Virology* **434**, 129–136 (2012).
62. L. J. Anderson, J. C. Hierholzer, Y. O. Stone, C. Tsou, B. F. Fernie, Identification of epitopes on respiratory syncytial virus proteins by competitive binding immunoassay. *J. Clin. Microbiol.* **23**, 475–480 (1986).

Acknowledgments: We thank T. Jain for guidance on statistical analyses, T. Boland for assistance with antibody sequence analysis, E. Shipman for assistance with protein expression, W. Li for technical assistance, C. Williams and S. M. Eagol for assistance with figure preparation, and M. Ackerman for use of the magnetic microplate washer (BioTek) and the FLEXMAP 3D flow cytometer (Luminex). PBMC processing was carried out in DartLab, the Immune Monitoring and Flow Cytometry Shared Resource, supported by a National Cancer Institute Cancer Center Support Grant to the Norris Cotton Cancer Center (P30CA023108-37) and an Immunology COBRE Grant (P30GM103415-15) from the National Institute of General Medical Sciences. All the IgGs were sequenced by Adimab's Molecular Core and produced by the High Throughput Expression group. Biolayer interferometry binding experiments were performed by Adimab's protein analytics group. **Funding:** Support for this work was provided by the National Institute of General Medical Sciences of the NIH awards T32GM008704 (M.S.A.G.) and P20GM113132 (J.S.M.) and by intramural funding from the National Institute of Allergy and Infectious Diseases to support work at the Vaccine Research Center (B.S.G.). This work was partially supported by grant SAF2015-67033-R to J.A.M. from Plan Nacional I+D+i. **Author contributions:** L.M.W., M.S.A.G., and J.S.M. wrote the manuscript. L.M.W., J.S.M., P.F.W., J.A.M., and B.S.G. analyzed the results, edited the manuscript, and provided intellectual oversight. C.A.C., M.S.A.G., M.C., J.O.N., L.M.W., S.M.M., V.M., and E.G. planned and performed the experiments. L.M.W. performed the statistical analyses. **Competing interests:** L.M.W. is an inventor on pending patent applications describing the RSV antibodies ("Anti-respiratory syncytial virus antibodies, and methods of their generation and use," USSN 62/411,500, USSN 62/411,508, and USSN 62/411,510). M.C., J.S.M., and B.S.G. are inventors on patent applications regarding prefusion-stabilized F proteins and their use ("Prefusion RSV F proteins and their use," PCT/US2014/026714). L.M.W., C.A.C., and E.G. have an equity position in Adimab LLC. The other authors declare that they have no competing interests. **Data and materials availability:** GenBank accession numbers for the antibody variable region gene sequences reported in this study can be found in data file S1.

Submitted 9 September 2016

Accepted 14 November 2016

Published 9 December 2016

10.1126/scimmunol.aa1879

Citation: M. S. A. Gilman, C. A. Castellanos, M. Chen, J. O. Ngwuta, E. Goodwin, S. M. Moin, V. Mas, J. A. Melero, P. F. Wright, B. S. Graham, J. S. McLellan, L. M. Walker, Rapid profiling of RSV antibody repertoires from the memory B cells of naturally infected adult donors. *Sci. Immunol.* **1**, eaaj1879 (2016).

Rapid profiling of RSV antibody repertoires from the memory B cells of naturally infected adult donors

Morgan S. A. Gilman, Carlos A. Castellanos, Man Chen, Joan O. Ngwuta, Eileen Goodwin, Syed M. Moin, Vicente Mas, José A. Melero, Peter F. Wright, Barney S. Graham, Jason S. McLellan and Laura M. Walker

Sci. Immunol. 1, (2016)
doi: 10.1126/sciimmunol.aaj1879

Editor's Summary Respiratory syncytial virus (RSV) causes cold-like symptoms in healthy adults but can have serious complications in both the very young and elderly. No vaccine is approved for RSV, and although a prophylactic antibody, palivizumab, is available for high-risk infants, therapy is generally supportive. Now, Gilman et al. profile the human antibody response to the RSV fusion (F) glycoprotein. They find that the response is broad but that more potent antibodies tend to target the apex of the prefusion conformation of RSV F, suggesting this site as a putative vaccine target. Moreover, many of these antibodies were more potent than palivizumab and some cross-neutralized human metapneumovirus, making them candidates for new passive prophylactics.

You might find this additional info useful...

This article cites 60 articles, 32 of which you can access for free at:

<http://immunology.science.org/content/1/6/eaaj1879.full#BIBL>

Updated information and services including high resolution figures, can be found at:

<http://immunology.science.org/content/1/6/eaaj1879.full>

Additional material and information about **Science Immunology** can be found at:

<http://www.sciencemag.org/journals/immunology/mission-and-scope>

This information is current as of December 10, 2016.